Analysis and mitigation of phase noise and sampling jitter in OFDM radio receivers

VILLE SYRJÄLÄ AND MIKKO VALKAMA

This article addresses the analysis and digital signal processing (DSP)-based mitigation of phase noise and sampling clock jitter in orthogonal frequency division multiplexing (OFDM) radios. In the phase noise studies, the basic direct-conversion receiver architecture case is assumed with noisy downconverting oscillator. In the sampling jitter case, on the other hand, the so-called direct-radio-frequency-sampling receiver architecture is deployed utilizing bandpass sub-sampling principle. The basis for the DSP-based impairment mitigation techniques is first formed using analytical receiver modeling with incoming OFDM waveform, where the effects of both oscillator phase noise and sampling clock jitter are mapped to certain type subcarrier cross-talk and distortion compared to ideal receiver case. Then iterative detection principles and interpolation techniques are developed to essentially estimate and cancel the subcarrier distortion. Also some related practical aspects, like channel estimation, are addressed. The performance of the proposed mitigation techniques is analyzed and verified with extensive computer simulations. In the simulations, realistic phase-locked-loop-based oscillator models are used for phase noise and sampling clock jitter. In addition, different received signal conditions like plain additive white Gaussian noise channel and extended ITU-R Vehicular A multipath channel are considered for practical purposes. Altogether the obtained results indicate that the effects of oscillator and sampling clock instabilities can be efficiently reduced using the developed signal processing techniques.

I. INTRODUCTION

In recent years, raw processing power of mobile radios has been greatly increasing. This has allowed implementation of various computationally intensive digital signal processing (DSP) stages in radios, e.g., for data detection and decoding purposes to improve the overall receiver and link performance [1]. In addition, by using the available DSP power, some nonidealities of the used radio frequency (RF) electronics can be reduced, enabling the use of cheaper, smaller, and less power consuming analog radio components [1]. Good examples are, e.g., power amplifier linearization, I/Q imbalance compensation, reduction of mixer nonlinearities, just to name a few [1]. Due to the above-mentioned rapid advances in digital implementation techniques, the available processing power has risen while also lowering the costs, size, and power consumption of the usable processing units at the same time. On the analog/RF electronics side, on the other hand, the main trend is the miniaturization of the integrated circuitry.

Oscillator is one of the most fundamental analog components used in almost every radio. On the implementation side, the random fluctuations of the instantaneous phase and frequency of the generated oscillator signal are called phase noise, which can cause many problems in novel and future communications systems and the corresponding radio

Department of Communications Engineering, Tampere University of Technology, Tampere, Finland.
Corresponding author:
V. Syrjälä
Email: ville.syrjala@tut.fi

devices [2–5]. In the earlier systems and their device implementations, stemming typically from the single carrier modulation principle combined with the use of superheterodyne or direct-conversion radio architectures, phase noise was hardly a problem. Nowadays, however, the effects of phase noise can be much more severe, since the used waveforms are getting more complex (and thus sensitive to any additional distortion), and also because less receiver selectivity is typically implemented at RF, compared to earlier device implementations. Most emerging radio systems are based on multicarrier modulation, mainly orthogonal frequency division multiplexing (OFDM) or some of its variants. OFDM-type waveforms have generally a fair amount of advantages over the more traditional single carrier signals [6], but there is also price to pay since multicarrier systems are found relatively vulnerable to radio component non-idealities, such as phase noise [2]. This is one of the main themes of this article. Phase noise effect on OFDM waveforms, in terms of in-band distortion, is generally twofold [2]. First of all, it causes rotation of symbol constellation called common phase error (CPE). This effect is very similar to the phase noise effect on single carrier systems, and is thus fairly easily canceled. However, the second effect, namely inter-carrier interference (ICI), is the spread of the subcarriers on top of each other. This is a very complex process by nature and its cancelation is not a simple task anymore [7], because the effect is varying from subcarrier to another.

As already mentioned, traditionally superheterodyne and direct-conversion receiver architectures have been widely used in mobile receivers. However, in order to reduce the size, cost, and power consumption of the receiver while increasing flexibility and re-configurability, the so-called direct-RF-sampling

(DRFS) receiver principle has received much attention in the research community (see, e.g., [8] and the references therein). In theory, the idea is simply to sample the incoming radio signal as near to the antenna as possible, using bandpass sampling principle [9, 10]. This, however, is not as simple as it sounds, as it causes very tight requirements for the sampling process, especially if the RF filtering is implemented in any realistic manner. Stemming from the high-frequency nature of the incoming signal, with high rate of change on the time axis, one of the biggest obstacles is the needed timing accuracy in the sampling process [11]. In practice, these sampling instants are determined by the sampling clock. As any oscillating type signals, also the clock signals are inherently noisy, thus causing inaccuracies in the sampling instants called sampling jitter [12].

This article focuses on the understanding and DSP-based reduction of phase noise and sampling jitter in OFDM receivers. In the literature, phase noise mitigation in OFDM systems has already been quite widely studied, e.g., in [7, 13–18]. In [7, 13, 14], the current state-of-the-art techniques are proposed, utilizing iterative detection principles. Sampling jitter mitigation, in turn, has also received some attention in the recent literature, e.g., in [19–21]. Especially for DRFS receivers, in [19, 20], the state-of-the-art techniques for sampling jitter cancelation are given for OFDM systems and for general communications systems, respectively. In this article, DSP methods to cancel phase noise-like phenomena in OFDM systems are further developed and studied. General ICI cancellation methods utilizing iterative detection and interpolation at multicarrier symbol boundaries are developed for reducing the phase noise effects in direct-conversion receivers. Also practical aspects, like channel estimation, are addressed. In addition, we show that it is possible to use the developed phase noise mitigation methods also for sampling jitter cancelation in DRFS type receivers, because the phase noise and sampling jitter phenomena are eventually quite similar. This is shown analytically and further verified using simulations. Comprehensive performance simulations are also generally used to assess the performance of the developed methods, using 3GPP-LTE-like system as a practical example.

Layout of the rest of the paper is as follows. Section II gives OFDM system modeling under the influence of phase noise in direct-conversion receivers. In addition, sampling jitter is studied in DRFS receiver and the phase noise-like effect of the sampling jitter is established. In Section III, the used PLL-based oscillator model is shortly described. Then, Section IV introduces the phase noise mitigation techniques with detailed descriptions of the needed signal processing. Section V depicts the simulation environment used to evaluate the performance of the studied techniques, and gives and analyzes the obtained simulation results. The work is concluded in Section VI.

II. PHASE NOISE AND SAMPLING JITTER IN OFDM RECEIVERS

In this section, the system modeling for phase noise in direct-conversion receiver and sampling jitter modeling for DRFS receivers are given.

A) Phase noise in direct-conversion receiver

OFDM symbols that consist of N subcarriers can be constructed using inverse discrete Fourier transform of length N on vector of same length loaded with complex subcarrier symbols. The corresponding time-domain samples of an individual OFDM symbol can thus be formulated as

$$x_m(n) = \frac{1}{\sqrt{N}} \sum_{k=0}^{N-1} X_m(k) e^{j2\pi nk/N}, \qquad (1)$$

where $X_m(k)$ denotes the kth subcarrier data symbol in mth OFDM symbol. In practice, OFDM systems usually implement also a so-called cyclic prefix, which is basically copying the last samples of each OFDM symbol before the first samples. The resulting OFDM symbol is then transmitted using I/Q modulation at desired center frequency. On the receiver side, after traveling through the noisy multipath channel, the signal is I/Q downconverted, filtered, and sampled. Assuming the phase noise process of the downconverting oscillator is denoted by $\phi(t)$, and that the cyclic prefix is longer than the channel delay spread, the received samples corresponding to (1), written in vector form, are given by

$$\mathbf{y}_m = \text{diag}(e^{j\boldsymbol{\phi}_m})(\mathbf{h}_m \otimes \mathbf{x}_m) + \mathbf{n}_m. \qquad (2)$$

Here, $\otimes$ is a circular convolution operator, $\mathbf{x}_m$ is the vector of samples of mth transmitted OFDM symbol in (1), $\mathbf{h}_m$ is the channel impulse response vector, and $\mathbf{n}_m$ is additive white Gaussian noise (AWGN) vector, all at mth OFDM symbol duration. In addition, $\boldsymbol{\phi}_m$ contains the samples of the phase noise realization within mth OFDM symbol, so $\boldsymbol{\phi}_m = [\phi_m(0), \ldots, \phi_m(N-1)]^T$.

After reception of the signal, OFDM-demodulation is done by using discrete Fourier transform giving frequency domain version of (2) as

$$\begin{aligned} \mathbf{Y}_m &= \mathbf{J}_m^{pn} \otimes (\mathbf{H}_m \bullet \mathbf{X}_m) + \boldsymbol{\eta}_m \\ &= \mathbf{J}_m^{pn} \otimes \mathbf{S}_m + \boldsymbol{\eta}_m, \end{aligned} \qquad (3)$$

where $\bullet$ is an element-wise multiplication operator, $\mathbf{X}_m$ is the vector of transmitted subcarrier symbols, $\mathbf{H}_m$ is the channel transfer function, $\boldsymbol{\eta}_m$ is the discrete Fourier transform (DFT) of AWGN, $\mathbf{S}_m = \mathbf{H}_m \bullet \mathbf{X}_m$, and finally $\mathbf{J}_m^{pn}$ is the DFT of the phase noise exponential $\exp(j\boldsymbol{\phi}_m)$, again all at mth OFDM symbol duration. This vector $\mathbf{J}_m^{pn}$ is referred to as the ICI profile in the following, and its elements can also be written explicitly as

$$J_m^{pn}(k) = \frac{1}{\sqrt{N}} \sum_{n=0}^{N-1} e^{j\phi_m(n)} e^{-j2\pi nk/N}. \qquad (4)$$

As mentioned previously, phase noise impact on OFDM system can be divided into two fundamentally different effects, CPE and ICI. These effects can now be quantified by writing the observation at subcarrier k (i.e., kth element of vector $\mathbf{Y}_m$ given in (3)) as

$$\begin{aligned} Y_m(k) = {} & J_m^{pn}(0) H_m(k) X_m(k) \\ & + \sum_{l=0, l \neq k}^{N-1} H_m(l) X_m(l) J_m^{pn}(k-l) + \eta_m(k). \end{aligned} \qquad (5)$$

In (5), the received subcarrier signal is divided into two parts, in first of which $J_m^{pn}(0)$ multiplies the interesting signal

(transmit symbol after channel response). This multiplication is the already mentioned CPE effect of the phase noise. The ICI effect of phase noise, in which the OFDM subcarriers are spread over top of each other, is seen as the second term on the right-hand side of (5).

B) Sampling jitter in direct-RF-sampling receiver

Since in the DRFS receiver, the sampling takes place already at high frequencies, also the modeling needs to reflect the bandpass nature of the actual RF signals. For generality, let us consider a general I/Q modulated bandpass waveform of the form

$$r(t) = s_I(t) \cos(2\pi f_c t) - s_Q(t) \sin(2\pi f_c t). \qquad (6)$$

Here $s_I(t)$ and $s_Q(t)$ denote the I- and Q-components of the received signal, respectively, and f_c is the corresponding formal center frequency. Notice that the exact structure of the I- and Q-components depend on the assumed RF filtering, i.e., they can model either a single communication waveform (desired signal) or more generally contain also the neighboring channels. Now, if sampling is directly applied to the above general bandpass signal with a jittered sampling clock, the corresponding jittered samples read

$$\begin{aligned} r_n &= r(nT_s + \zeta_n) \\ &= s_I(nT_s + \zeta_n) \cos[2\pi f_c(nT_s + \zeta_n)] \\ &\quad - s_Q(nT_s + \zeta_n) \sin[2\pi f_c(nT_s + \zeta_n)]. \end{aligned} \qquad (7)$$

Here the jittered sample instants are denoted by $t_n = nT_s + \zeta_n$, where ζ_n models the uncertainty of the nth sample instant and T_s is the nominal sampling interval. In this presentation, it is obvious that the jitter implicitly affects both the samples of low-frequency useful signal components (s_I and s_Q), and the high-frequency carrier components (sine and cosine waves). In any realistic received signal scenario, however, the frequency range of the carrier components is in the order of 100–1000 times higher compared to the modulating I and Q components. This means that the sampling jitter has much more significant effect on the carrier components of the signal than on the useful (modulating) part of the signal. Thus for any realistic jitter level, we can basically approximate (7) by

$$\begin{aligned} r_n &= r(nT_s + \zeta_n) \\ &\approx s_I(nT_s) \cos[2\pi f_c(nT_s + \zeta_n)] \\ &\quad - s_Q(nT_s) \sin[2\pi f_c(nT_s + \zeta_n)]. \end{aligned} \qquad (8)$$

Note that because an arbitrary bandpass signal was assumed in the above derivations, the result in (8) can be deployed in modeling sampling jitter in any realistic bandpass system, independently of the exact communication waveforms used.

Next, we deploy the basic modeling result in (8) and develop it further for DRFS receiver purposes by assuming that the sub-sampling principle [10] is utilized in the receiver implementation. In effect, this means that aliasing is used in a controlled manner to downconvert the received signal to lower frequencies within the sampling process. In such case, $F_s = 1/T_s \ll f_c$ and (8) can be rewritten as

$$\begin{aligned} r_n &\approx s_I(nT_s) \cos[2\pi f_{IF} nT_s + 2\pi f_c \zeta_n] \\ &\quad - s_Q(nT_s) \sin[2\pi f_{IF} nT_s + 2\pi f_c \zeta_n] \\ &= \mathrm{Re}\{[s_I(nT_s) + js_Q(nT_s)]e^{j2\pi f_{IF} nT_s} e^{j2\pi f_c \zeta_n}\}. \end{aligned} \qquad (9)$$

Here, f_{IF} denotes the new aliased center frequency due to sub-sampling. Now, because we are already in digital domain, we can use complex digital mixing from IF to baseband, followed by lowpass filtering, which essentially yields

$$\begin{aligned} y_n &\approx [s_I(nT_s) + js_Q(nT_s)]e^{j2\pi f_c \zeta_n} \\ &= s_n e^{j2\pi f_c \zeta_n} \\ &= s_n e^{j\theta_n}, \end{aligned} \qquad (10)$$

where $s_n = s_I(nT_s) + js_Q(nT_s)$ and $\theta_n = 2\pi f_c \zeta_n$. This basically means that we can approximate the sampling jitter effect in DRFS receiver for general bandpass signal just as a multiplication by a complex exponential, just like the phase noise is modeled in general. Here, instead of the phase noise term ϕ induced by the downconversion stage in the earlier direct-conversion receiver case, we simply have a sampling jitter-dependent phase noise term $\theta_n = 2\pi f_c \zeta_n$ as the argument of the multiplying complex exponential. Thus based on the earlier developments in Section II.A, if OFDM waveforms are again assumed, sampling jitter in DRFS receiver will essentially again result in CPE and ICI-type distortions. Thus using similar notations as in Section II.A, the subcarrier observations at mth OFDM symbol duration can be written as

$$\begin{aligned} \mathbf{Y}_m &= \mathbf{J}_m^{jit} \otimes (\mathbf{H}_m \bullet \mathbf{X}_m) + \boldsymbol{\eta}_m \\ &= \mathbf{J}_m^{jit} \otimes \mathbf{S}_m + \boldsymbol{\eta}_m. \end{aligned} \qquad (11)$$

Here $\mathbf{J}_m^{jit}$ denotes the DFT of the jitter-induced phase noise exponential within the mth OFDM symbol duration. This observation will be utilized in the actual ICI mitigation developments in Section IV.

III. OSCILLATOR MODELING

In this section, the used oscillator phase noise modeling is shortly addressed. In general, phase noise modeling stems from physical circuit-level analysis or empirical studies. One of the most simple models widely applied in the literature is the so-called free-running oscillator (FRO) model where the oscillator excess phase (phase noise) is assumed to follow the Brownian motion (Wiener process). This basically means that the phase error process is changing from sample to sample by an amount dictated by some variance parameter which, in turn, depends on the 3 dB bandwidth of the oscillator [3]. Effectively, the sampled phase noise process can thus be modeled as a cumulative sum of Gaussian distributed white noise variables whose variance is given by the quality of the oscillator. In this paper, however, more realistic phase-locked-loop (PLL)-based oscillators are considered to emphasize practicality. For simplicity, the same PLL model is used as a basis for both downconversion phase noise, in case of direct-conversion RX,

and sampling clock jitter, in case of DRFS receiver. In the modeling of the sampling jitter, the phase noise realization is normalized to have currently interesting jitter root-mean-square (RMS) value.

The exact PLL modeling in this paper is based on the one developed by the authors in [22]. In [22] the formulae for deriving the overall oscillator spectrum are derived and explained in detail, and are thus ignored here for simplicity. In the model, oscillator properties can be tuned through inputting phase noise spot measurement values of voltage-controlled and reference oscillators (VCO and RO) used inside the PLL. These spot measurement values characterize the phase noise power-spectral density of the VCO and RO used in the corresponding PLL implementation.

The deployed PLL model derives the actual phase noise samples (elements of vector ϕ_m) in three steps: (i) complex Gaussian white noise is generated and Fourier transformed to frequency domain, (ii) frequency-domain noise is shaped by the phase noise mask derived according to the derived specifications in [22], and (iii) the shaped frequency domain noise is transferred back to time domain using inverse Fourier transform giving the phase noise vector ϕ_m. The actual phase noise mask of the PLL-based oscillator used in this paper is depicted in Fig. 1. The same phase noise model was also used in [13]. The exact spot measurement values used are as follows. For VCO, $1/f$-noise-dominated region measurement at 30 kHz offset from the oscillation frequency is -75 dBc/Hz and the thermal-noise-dominated region measurement at 1 MHz offset is -110 dBc/Hz. For reference oscillator, we assume that no meaningful flicker noise is present and that the thermal-noise region measurement at 100 Hz offset is -90 dBc/Hz. Note that these used PLL specs are of course simply one specific example but anyway represent realistic and practical PLL design.

IV. PHASE NOISE AND SAMPLING JITTER MITIGATION

In this section, the actual digital mitigation techniques to reduce the effects of phase noise and sampling jitter are developed, stemming from the previous receiver modeling in Section II. Here we mostly focus on the ICI cancelation because the CPE
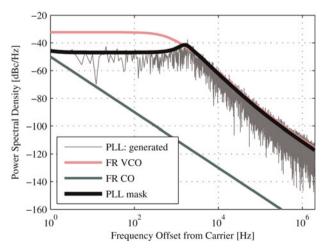

Fig. 1. Example phase noise mask and its underlying components depicted with actual generated PLL-oscillator spectrum centered at 2 GHz.

part is fairly well managed in the literature. These CPE mitigation techniques typically assume ICI to be just additional noise and, e.g., least-squares (or zero forcing) principle is used to estimate the CPE [17] using pilots. CPE mitigation is then done just by inverse rotation of the constellation.

In the following, we focus on the ICI estimation and cancelation. Notice that given the ICI profile ($\mathbf{J}_m$), the actual mitigation can be done by deploying circular deconvolution between the estimated ICI profile and the observed subcarrier samples $\mathbf{Y}_m$, as (3) and (11) imply. This results in the estimate of $\mathbf{S}_m = \mathbf{H}_m \cdot \mathbf{X}_m$, and can be written as

$$\hat{\mathbf{S}}_m = (\mathbf{P}\hat{\mathbf{J}}_m^*) \otimes \mathbf{Y}_m, \qquad (12)$$

where $\hat{\mathbf{J}}_m$ denotes the ICI profile estimate, $\mathbf{P}$ is a permutation matrix that reverses the order of elements in the vector that it multiplies, and $(\cdot)^*$ denotes complex conjugation. Note that due to the structural similarity of the effect of phase noise and sampling jitter in direct-conversion and DRFS receivers, respectively, we do not differentiate those two in the mitigation processing descriptions below, but simply refer to both of them as phase noise. Also the simplified notation $\mathbf{J}_m$ is used for the ICI profile, instead of $\mathbf{J}_m^{pn}$ and $\mathbf{J}_m^{jit}$. In below, we first describe in Section IV.A state-of-the-art reference technique developed in [7]. Then the proposed technique is introduced in Section IV.B, discussed by the authors preliminary in [13]. Section IV.C then discusses the practical channel estimation aspects for the proposed technique.

A) ICI estimation technique of Petrovic *et al.*

To our knowledge, the best available technique for ICI estimation in the literature is the method proposed in [7] by Petrovic *et al.*, to which in this paper we simply refer as Petrovic's technique. In this approach, the idea is to estimate the most dominant frequency bins of the ICI profile. This is motivated by the typically observed steep slopes of the oscillator spectrum around the nominal oscillating frequency. This reduces the computational complexity of the estimation task in a considerable manner, yet not compromising the performance, compared to trying to estimate all the components of the ICI profile. The actual estimation is done by using initial subcarrier symbol decisions (with CPE mitigation only) as reference. To be more specific, given that we want to estimate the center frequency bin of $\mathbf{J}_m$ along with the u adjacent frequency bins on both sides, the system model given in (3) can be first reformulated into form

$$\begin{bmatrix} Y_m(l_1) \\ \vdots \\ Y_m(l_P) \end{bmatrix} = \begin{bmatrix} S_m(l_1+u) & \cdots & S_m(l_1-u) \\ \vdots & \ddots & \vdots \\ S_m(l_P+u) & \cdots & S_m(l_P-u) \end{bmatrix}$$

$$\times \begin{bmatrix} J_m(-u) \\ \vdots \\ J_m(u) \end{bmatrix} + \begin{bmatrix} \eta_m(l_1) \\ \vdots \\ \eta_m(l_P) \end{bmatrix} \qquad (13)$$

$$\Leftrightarrow$$

$$\mathbf{Y}_{m,p} = \mathbf{M}_{m,u}\mathbf{J}_{m,u} + \boldsymbol{\eta}_{m,p},$$

where $l_1, \ldots, l_P$ refer to used subcarriers in the estimation task. This model is obtained by simply picking the $l_1, \ldots, l_P$ rows from the model in (3) and writing the truncated circular

convolution as a matrix–vector product. Now, the elements $S_m(l) = H_m(l)X_m(k)$ of the matrix $\mathbf{M}_{m,u}$ above are first obtained using initial data detection (after CPE mitigation) combined with channel state information. Then, the ICI profile is estimated using, e.g., least-squares technique as

$$\hat{\mathbf{J}}_{m,u} = \left(\mathbf{M}_{m,u}^H \mathbf{M}_{m,u}\right)^{-1} \mathbf{M}_{m,u}^H \mathbf{Y}_{m,p}. \qquad (14)$$

Then we do the ICI mitigation, as given in (12), detect the data again and input the resulting detected subcarrier symbols to the ICI estimation algorithm again. This iterative estimation-mitigation technique is then run for a few iterations until no clear improvements in detection results are achieved. For more detailed information, refer to [7].

By the same research group, a way to further improve the above Petrovic's technique was proposed in [14] by Bittner *et al.* In [14], it was noted that the estimation method of [7] gives very poor phase noise estimation performance near the boundaries of OFDM symbols due to the truncated Fourier series approach used. This is why they introduced a technique to "shift" the phase noise effects so that the reliability of the tail parts of the estimates can be improved. For more details on this technique refer to [14]. This improved technique will be used as the main reference in performance evaluations in Section V.

B) Proposed linear interpolation – tail estimation (LI-TE) ICI-estimation technique

Also in [13], the poor estimation performance in the tail parts of the phase noise estimates given by the Petrovic's technique was noticed. In addition, it was noted that the continuous nature of the phase error in time domain can be exploited in the phase noise estimation process quite efficiently. This results in the so-called LI-TE technique which is described in details in the following.

The proposed LI-TE estimation technique builds on the earlier iterative ICI profile estimation scheme and improves the estimation performance of individual iterations by using interpolation over the phase noise estimates at OFDM symbol boundaries in which the initial phase noise estimates are poor. The whole procedure including the initial ICI detection done by Petrovic's technique is depicted in Tables 1 and 2 for the case of two iterations. Thus if the phase noise mitigation is started at the mth OFDM symbol, the initialization of the algorithm described in Table 1 is first deployed, and is then followed by the actual mitigation loop given in Table 2. For simplicity, the formulation is here given for two iterations but it is trivial to extend the algorithms to more than two iterations. Stemming from the interpolation principle, it should

Table 1. ICI estimation algorithm (LI-TE) – initialization.

Step	Action
1	CPE estimation and mitigation, and symbol detection for OFDM symbols m and $m+1$*
2	ICI estimation (14) for OFDM symbols m and $m+1$
3	Linear interpolation at symbol boundary between OFDM symbols m and $m+1$ (LI-TE)
4	Remove estimated phase noise and detect the OFDM symbol m

*Indicates the step where channel estimation is needed.

Table 2. ICI estimation algorithm (LI-TE) – mitigation loop.

Step	Action
1	CPE estimation and mitigation, and symbol detection for OFDM symbol $m+2$*
2	ICI estimation (14) for OFDM symbol $m+2$
3	Linear interpolation at symbol boundary between OFDM symbols $m+1$ and $m+2$ (LI-TE)
4	Remove estimated phase noise and detect the OFDM symbol $m+1$
5	ICI estimation (14) for OFDM symbols m and $m+1$
6	Linear interpolation at symbol boundary between OFDM symbols m and $m+1$ (LI-TE)
7	Remove estimated phase noise and detect the OFDM symbol m
8	Set $m = m+1$ and move to step 1

be acknowledged that the overall estimation–cancelation processing is subject to delay in the final detection. With two iterations, the delay is also two OFDM symbols. In general, adding one further iteration increases also the delay by one symbol.

Next, we consider the implementation of the interpolation stage. First let the interpolation window length for both sides of each OFDM symbol be denoted by L (samples). Then in the individual interpolation stage, the estimated ICI profile is transferred back to time-domain phase noise vector ϕ_m with simple IFFT and taking the angle of the complex exponential as

$$\hat{\boldsymbol{\phi}}_m = \arg\left\{\text{IFFT}\left[\hat{\mathbf{J}}_{m,u}\right]\right\}. \qquad (15)$$

Then, assuming that simple linear interpolation is used, the processing of the phase noise estimates at the boundary between OFDM symbols m and $m+1$ can be mathematically formulated as

$$
\begin{aligned}
\tilde{\boldsymbol{\phi}}_m(N-L+n) &= \hat{\boldsymbol{\phi}}_m(N-L) \\
&\quad + n\frac{\hat{\boldsymbol{\phi}}_{m+1}(L) - \hat{\boldsymbol{\phi}}_m(N-L)}{2L}, \\
\tilde{\boldsymbol{\phi}}_{m+1}(n) &= \hat{\boldsymbol{\phi}}_m(N-L) \\
&\quad + (L+n)\frac{\hat{\boldsymbol{\phi}}_{m+1}(L) - \hat{\boldsymbol{\phi}}_m(N-L)}{2L},
\end{aligned}
$$

$$(16)$$

where $\hat{\boldsymbol{\phi}}_m(n)$ refers to the nth sample of the initially estimated phase noise, at OFDM symbol m, whereas $\tilde{\boldsymbol{\phi}}_m(n)$ refers to the corresponding interpolated quantity. Note that the original time domain received signal contains also the cyclic prefix in the boundary area, but the cyclic prefix length is typically relatively small compared to the OFDM symbol length and phase error dynamics. This basically means that we can still consider the phase noise a continuous process, and thus interpolation over the badly estimated boundary regions will indeed improve the performance, as will be demonstrated below and in more details in Section V.

An example estimation result obtained with the proposed technique is depicted in Fig. 2. As demonstrated in Fig. 2, the use of interpolation does indeed greatly improve the quality of the phase noise estimates near OFDM symbol
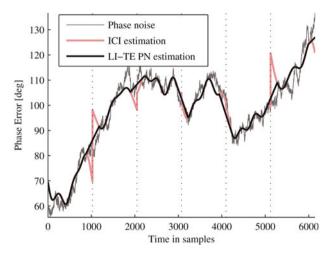
Fig. 2. LI-TE ICI-estimation technique interpolates over the peaking phase noise estimates of Petrovic's technique near the OFDM symbol boundaries. FRO is used with 100 Hz 3 dB bandwidth as an example. Estimation is done under 18 dB received signal conditions.

boundaries. Petrovic's basic ICI estimation technique causes bad peaking of the estimates near the boundaries, which is nicely smoothened by the interpolation stage. More detailed and quantitative performance assessments will be carried out in Section V.

C) Channel estimation aspects

If we do not have channel knowledge in the receiver by default, as is usually the case, we must also consider the channel estimation task in practice. In the iterative ICI estimation setup, already the initial detection needs (estimated) channel knowledge of some kind. Also when building and solving the linear model in (13) and (14), channel knowledge is required in constructing the matrix $\mathbf{M}_{m,u}$. Typically, pilot subcarriers are deployed for channel estimation in practical multicarrier systems. This is also assumed to be the case in the following.

One specific issue, due to the interpolation approach in ICI cancelation, is that the proposed LI-TE technique requires that the effective phase noise process is continuous at symbol boundaries. Now if the combined effect of CPE and multipath channel is estimated and equalized using pilot subcarriers, independently from one multicarrier symbol to another, this is actually not the case because the CPE can easily vary from multicarrier symbol to another. Thus, after equalizing the joint effect of channel and CPE, the continuous nature of the phase noise in the overall system is essentially lost.

However, the effect of CPE can actually be separated from the channel if a quasi-static channel is assumed. In such cases, the channel is assumed changing very slowly being thus virtually static for a period of say K OFDM symbols. This can then be exploited in channel estimation, when we want to recover (separate) the CPE information from the actual radio channel. In the channel estimation stage, pilot subcarriers are first used to estimate the combined response. For example, the zero forcing principle can be used, written as

$$\hat{\mathbf{H}}_{m,pilots} = \mathbf{Y}_{m,pilots} \bullet / \mathbf{P}_m, \qquad (17)$$

where $\bullet /$ is point-by-point division operator, $\mathbf{P}_m$ is vector of pilot subcarriers in mth OFDM symbol, and *pilots* sub-index

refers to subcarrier symbol indices that carry the pilot data. Now if we assume a quasi-static system, this and the channel estimates for the $K - 1$ OFDM symbols around the current symbol should be the same if there were no CPE in the system. So we can now easily estimate the relative CPEs (relative to one of the multicarrier symbols, say mth) by simply dividing the corresponding channel estimates by the channel estimate of the reference symbol, meaning

$$\hat{\mathbf{J}}^o_{l,rel} = \hat{\mathbf{H}}_{l,pilots} \bullet / \hat{\mathbf{H}}_{m,pilots}. \qquad (18)$$

Now, for each of the OFDM symbols within the processing window of K symbols, we have multiple relative CPE estimates in the vectors $\hat{\mathbf{J}}^o_{l,rel}$. By recognizing that CPE is, by definition, identical for all the subcarriers within single OFDM symbol, we can filter these multiple estimates to a more reliable estimate by, e.g., taking the mean value as

$$\hat{J}_{l,rel}(o) = \overline{\hat{\mathbf{J}}^o_{l,rel}}. \qquad (19)$$

In above, $\overline{\mathbf{x}}$ refers to sample mean of the elements of $\mathbf{x}$. The CPE can then be separated from the estimated channel by dividing the channel estimate vectors for each OFDM symbol by the corresponding CPE estimate in (19). Now, also the quasi-static assumption can be further deployed in actual channel estimation, because the remaining channel estimates do not have CPE (and should thus be constant at any given subcarrier from multicarrier symbol to another). Improved channel estimates can thus be achieved, e.g., simply by taking the mean of the channel estimates over the processing window. Finally, the channel estimates for active subcarriers are obtained using interpolation as in any typical multicarrier receiver. Note that length of the above processing window K is in practice limited by the assumed mobility of the receiver.

In the overall phase noise mitigation setup described in Tables 1 and 2, the channel estimation and the corresponding CPE recovery are carried out in steps marked with (*), namely before CPE is estimated and mitigated.

V. SIMULATION ENVIRONMENT AND OBTAINED RESULTS

In this section, the performances of the previously described phase noise mitigation techniques are studied, for both the case of phase noise mitigation in traditional direct-conversion receiver and the case of sampling jitter mitigation in DRFS receiver. Also the effects of channel estimation procedure are addressed.

A) Simulation parameters

In the simulations, 3GPP-LTE downlink-like [23] system is assumed for practicality, utilizing OFDM with 1024 subcarriers and 15 kHz subcarrier spacing, combined with cyclic prefix of length 63 samples. Of the 1024 subcarriers, 600 are active, 300 on the both sides of the zero-subcarrier. All the other subcarriers are empty (zeroed). 16QAM subcarrier modulation is assumed here for active subcarriers. Concerning the pilot allocation, 18 of the active subcarriers carry pilot data in the basic simulations where perfect

channel knowledge is first assumed. Then, in the simulations where also the channel response is estimated (in addition to ICI profile), every ninth subcarrier carries the pilot data to facilitate reasonable estimation performance.

The simulations are carried out as follows. First, 16QAM subcarrier data are generated and OFDM modulated, and the resulting OFDM signal is sent to the channel. Channel is either AWGN channel or extended ITU-R Vehicular A multipath [24] channel. The channel response is assumed constant for single simulation realization which always contains a packet of 12 OFDM symbols. In a new realization, also new channel response is drawn, and altogether a minimum of 5000 independent channel realizations are always simulated for a given SNR or jitter RMS point. After the channel, receiver phase noise or sampling jitter is applied, according to which case we study. The phase noise and sampling jitter are based on PLL-oscillator phase noise model discussed in Section III. After the impairment has been applied, impairment mitigation and detection are carried out, as explained in Section IV.

In all the iterative techniques, only two iterations are used for implementation simplicity. In ICI estimation, three frequency bins of the ICI profile on both sides of the DC-bin are estimated. For Bittner's technique, shifting window length is 70 samples of length and for LI-TE the interpolation window length L is 155 samples. The window lengths were chosen based on comparative performance simulations.

B) Phase noise mitigation performance in direct-conversion receiver case

In Figs 3 and 4, the performances of the presented mitigation techniques in phase noise corrupted OFDM direct-conversion receiver are given. Figure 3 depicts the performance in AWGN channel case. As can be seen, the ICI estimation techniques offer huge performance increase compared to if only CPE is mitigated. Furthermore, the LI-TE technique improves the performance quite noticeably over the Petrovic's and Bittner's techniques. From Fig. 4 one can see that as the channel gets more demanding, the overall system performance decreases heavily. This pushes the relative performance differences between the mitigation techniques close to each other, but at the same time, the mitigation curves are
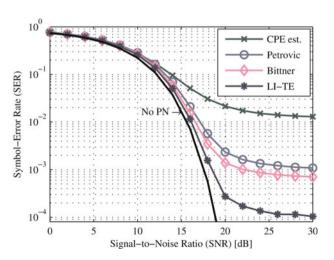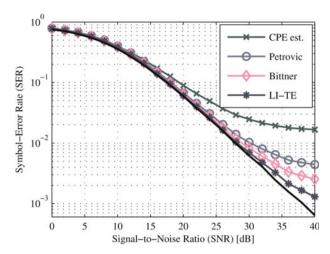
Fig. 4. SER given as a function of SNR with PLL-based oscillator phase noise in extended ITU-R Vehicular A multipath channel.

pushed closer and closer to the ideal performance curve. This happens naturally because the phase noise contribution to the system performance is a little smaller whereas the contribution of the channel gets more dominating. With more demanding oscillator models, the differences would naturally be higher.

Overall, the phase noise mitigation techniques work very well in the application they are intended for. The performances of all the ICI cancelation techniques are quite impressive, but the proposed LI-TE method is still showing clearly the best performance.

C) Sampling jitter mitigation performance in direct-RF-sampling receiver case

In Figs 5 and 6, the performances of phase noise mitigation techniques are depicted for sampling jitter mitigation in DRFS receiver with communications over AWGN channel. In the first study, the RMS jitter is fixed to 20 ps, and as shown in Fig. 5, all the mitigation techniques give very nice performance. While LI-TE gives a little better performance than the other techniques, all the ICI mitigation techniques
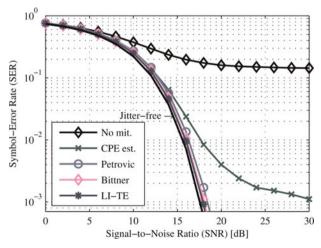
Fig. 3. SER given as a function of SNR with PLL-based oscillator phase noise in AWGN channel conditions.

Fig. 5. SER given as a function of SNR with PLL-oscillator shaped sampling jitter fixed at 20 ps RMS. AWGN channel is used.

give almost ideal performance. Next the studied RMS jitter range is widened up to 50 ps. Then, as Fig. 6 indicates, only LI-TE technique gives good performance over the whole studied region while the performance of other methods start to deteriorate fast when the RMS jitter is increased. Notice also that with RMS jitter values less than 15 ps, all the ICI mitigation techniques give almost the same performance and the performances of the techniques are pretty close to the no phase noise case.

From Figs 7 and 8 we can draw similar conclusions for the case with extended ITU-R Vehicular A multipath channel, as we did in the AWGN case. The total system performance is lowered quite noticeably, but the relative differences between the mitigation techniques stay unchanged. It is noticeable though that in AWGN case the SER got so low that the high-SNR region was not visible for the ICI mitigation techniques in the figures. However, with more challenging channel conditions, one can see that differences between the techniques start to get bigger and bigger as the SNR rises. In addition one can see that as the SNR gets very high, the performances of the mitigation techniques start to stabilize to some flooring levels, as was also observed in the earlier phase noise mitigation studies. However, this does not happen with practical SNR values from mobile communications point of view, at least for extended Vehicular A multipath channel.

D) Phase noise mitigation performance in direct-conversion receiver without perfect channel knowledge

Finally, we study the mitigation performance in cases where no prior knowledge of the channel state (response) is available, which is usually the case in practice. For simplicity, we focus on the direct-conversion receiver case. Figure 9 demonstrates the obtained performances under ITU-R Vehicular A multipath channel with two different channel estimation ideologies. The first one is conventional one-shot estimation using pilot subcarriers, which is carried out separately for each multicarrier symbol and interpolated inside each multicarrier symbol for the responses at active data carriers. This obviously suffers from the ICI due to phase noise. The second scheme is the one described in Section IV.C where the assumed quasi-static nature of the channel response is
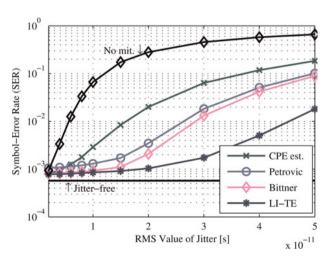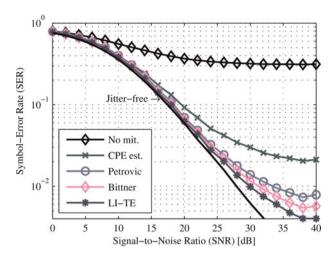

Fig. 7. SER given as a function of SNR with PLL-oscillator shaped sampling jitter fixed at 20 ps RMS. Extended ITU-R Vehicular A multipath channel is used.

taken advantage of. As Fig. 9 shows, the more advanced channel estimation scheme gives very good performance boost over the conventional channel estimations case with all the simulated techniques. With conventional channel estimation, the LI-TE technique does not work as planned because the technique needs the phase noise to act as a continuous process over the period longer than on OFDM symbol, as was discussed earlier. When the proposed channel estimation is applied, the LI-TE technique outperforms the Bittner's and Petrovic's techniques. In general, the performances stay somewhat behind the case with perfect channel knowledge which is unavoidable with any reasonable channel estimation scheme.

VI. CONCLUSIONS

Oscillator impairments such as phase noise and sampling jitter can easily degrade the performance of OFDM system in a considerable manner. In this paper, we presented state-of-the-art mitigation techniques for reducing the effects of oscillator impairments on the receiver side. Two
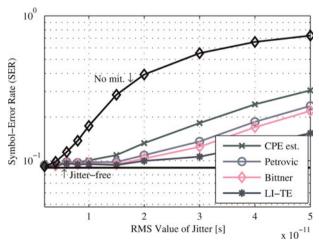

Fig. 6. SER given as a function of RMS jitter. Jitter is shaped by PLL-oscillator. AWGN channel conditions are used with fixed received SNR of 18 dB.

Fig. 8. SER given as a function of RMS jitter. Jitter is shaped by PLL-oscillator. Extended ITU-R Vehicular A multipath channel conditions are used with fixed received SNR of 18 dB.
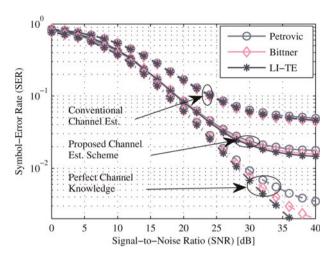
Fig. 9. SER given as a function of SNR with PLL-based oscillator phase noise in extended ITU-R Vehicular A multipath channel. Different levels of prior channel information are studied.

receiver topologies, namely the direct-conversion receiver architecture as well as the DRFS receiver architecture, were considered in more details and analyzed from the phase noise and sampling jitter points of view. Stemming from the modeling, the waveform distortion in both receiver architectures results in certain cross-talk between the OFDM subcarriers. Then generic cross-talk cancelation techniques were presented for mitigation of both sampling jitter as well as phase noise in the considered receiver architectures. It was further demonstrated with the help of simulations that the considered mitigation techniques perform very well under practical phase noise and sampling jitter conditions. Also the channel state information and estimation aspects were addressed. Overall, with practical PLL-based oscillators and practical RMS jitter values, the proposed LI-TE ICI estimation cancelation technique was shown to perform best reducing the signal distortion due to considered oscillator nonidealities in a considerable manner.

REFERENCES

[1] Fettweis, G.: Dirty RF: A new paradigm, in Proc. 16th Int. Symp. on Personal, Indoor and Mobile Radio Communications 2005, vol. **4**, September 2005, 2347–2355.

[2] Robertson, P. and Kaiser, S.: Analysis of the effects of phase-noise in orthogonal frequency division multiplex (OFDM) systems, in Proc. IEEE Int. Conf. on Communications, vol. **3**, June 1995, 1652–1657.

[3] Schenk, T.: RF Impairments in Multiple Antenna OFDM: Influence and Mitigation, Ph.D. Dissertation, Technische Universiteit Eindhoven, 2006, ISBN 90–386-1913-8, 291pp.

[4] Armada, A.; Calvo, M.: Phase noise and sub-carrier spacing effects on the performance of an OFDM communication system. IEEE Commun. Lett., **2** (1) (1998), 11–13.

[5] Tomba, L.: On the effect of Wiener phase noise in OFDM systems. IEEE Trans. Commun., **46** (5) (1998), 580–583.

[6] Bingham, J.A.C.: Multicarrier modulation for data transmission: an idea whose time has come. IEEE Commun. Mag., **28** (5) (1990), 5–14.

[7] Petrovic, D.; Rave, W.; Fettweis, G.: Effects of phase noise on OFDM systems with and without PLL: characterization and compensation. IEEE Trans. Commun., **55** (8) (2007), 1607–1616.

[8] Razavi, B.: RF Microelectronics, Prentice Hall PTR, Upper Saddle River, NJ, USA, 1998, 335pp.

[9] Frerking, M.E.: Digital Signal Processing in Communication Systems, International Thomson Publishing Services, 1994, 644pp.

[10] Vaughan, R.G.; Scott, N.L.; White, D.R.: The theory of bandpass sampling. IEEE Trans. Signal Process., **39** (1991), 1973–1984.

[11] Amin, B.; Dempster, A.G.: Sampling and jitter considerations for GNSS software receivers, in Proc. IGNSS Symp. 2006, July 2006, 15pp.

[12] Shinagawa, M.; Akazawa, Y.; Wakimoto, T.: Jitter analysis of high-speed sampling systems. IEEE J. Solid State Circuits, **25** (1) (1990), 220–224.

[13] Syrjälä, V.; Valkama, M.; Tchamov, N.N.; Rinne, J.: Phase noise modelling and mitigation techniques in OFDM communications systems, in Proc. Wireless Telecommunications Symp. 2008, Prague, Czech Republic, April 2009.

[14] Bittner, S.; Zimmermann, E.; Fettweis, G.: Exploiting phase noise properties in the design of MIMO-OFDM receivers, in Proc. IEEE Wireless Communications and Networking Conf. 2008, Las Vegas, NV, March 2008, 940–945.

[15] Bittner, S.; Rave, W.; Fettweis, G.: Joint iterative transmitter and receiver phase noise correction using soft information, in Proc. IEEE Int. Conf. on Communications 2007, June 2007, 2847–2852.

[16] Zou, Q.; Tarighat, A.; Sayed, A.H.: Compensation of phase noise in OFDM wireless systems. IEEE Transactions on Signal Processing, **55** (11) (2007), 5407–5424.

[17] Wu, S.; Bar-Ness, Y.: A phase noise suppression algorithm for OFDM-based WLANs. IEEE Commun. Lett., **6** (12) (2002), 535–537.

[18] Wu, S.; Bar-Ness, Y.: OFDM systems in the presence of phase noise: Consequences and solutions. IEEE Trans. Commun., **52** (11) (2004), 1988–1997.

[19] Syrjälä, V.; Valkama, M.: Jitter mitigation in high-frequency bandpass sampling OFDM radios, in Proc. IEEE Wireless Communications and Networking Conf. 2009, Budapest, Hungary, April 2009.

[20] Syrjälä, V.; Valkama, M.: Sampling jitter estimation and mitigation in direct RF sub-sampling receiver architecture, in Proc. Sixth Int. Symp. on Wireless Communication Systems 2009, Siena-Tuscany, Italy, September 2009.

[21] Rutten, R.; Breems, L.J.; van Veldhoven, R.H.M.: Digital jitter-cancellation for narrowband signals, in Proc. IEEE Int. Symp. on Circuits and Systems 2008, May 2008, 1444–1447.

[22] Tchamov, N.N.; Rinne, J.; Syrjälä, V.; Valkama, M.; Zou, Y.; Renfors, M.: VCO phase noise trade-offs in PLL design for DVB-T/H receivers, in Proc. IEEE Int. Conf. on Electronics Circuits and Systems 2009, December 2009.

[23] 3GPP Technical Specification, TS 36.211 v8.3.0, Physical Channels and Modulation (release 8), May 2008.

[24] Sorensen, T.B.; Mogersen, P.E.; Frederiksen, F.: Extension of the ITU channel models for wideband (OFDM) systems, in Proc. IEEE Vehicular Technology Conf., Fall-2005, Dallas, TX, September 2005, 392–396.

Ville Syrjälä was born in Lapua, Finland, on August 23, 1982. He received the M.Sc. degree (with honours) in communications engineering (CS/EE) from Tampere University of Technology (TUT), Finland, in 2007. Currently, he is working as a researcher with the Department of Communications Engineering at TUT, Finland. His general research interests are in communications signal processing and signal processing algorithms for flexible radios.

Mikko Valkama was born in Pirkkala, Finland, on November 27, 1975. He received the M.Sc. and Ph.D. degrees (both with honours) in electrical engineering (EE) from Tampere University of Technology (TUT), Finland, in 2000 and 2001, respectively. In 2002 he received the Best Ph.D. Thesis – award by the Finnish Academy of Science and Letters for his dissertation entitled "Advanced I/Q signal processing for wideband receivers: Models and algorithms." In 2003, he was working as a visiting researcher with the Communications Systems and Signal Processing Institute at SDSU, San Diego, CA. Currently, he is a Full Professor at the Department of Communications Engineering at TUT, Finland. He has been involved in organizing conferences, like the IEEE SPAWC'07 (Publications Chair) held in Helsinki, Finland. His general research interests include communications signal processing, estimation and detection techniques, signal processing algorithms for software defined flexible radios, digital transmission techniques such as different variants of multicarrier modulation methods and OFDM, and radio resource management for *ad hoc* and mobile networks.